Acta Neuropathologica (2018) 136:901–917
https://doi.org/10.1007/s00401-018-1922-z

ORIGINAL PAPER

Evidence of intraneuronal Aβ accumulation preceding tau pathology in the entorhinal cortex

Lindsay A. Welikovitch[1] · Sonia Do Carmo[2] · Zsófia Maglóczky[3] · Péter Szocsics[3] · János Lőke[4] · Tamás Freund[5] · A. Claudio Cuello[1,2,6]

Received: 13 September 2018 / Revised: 18 October 2018 / Accepted: 18 October 2018 / Published online: 25 October 2018

Abstract

Growing evidence gathered from transgenic animal models of Alzheimer's disease (AD) indicates that the intraneuronal accumulation of amyloid-β (Aβ) peptides is an early event in the AD pathogenesis, producing cognitive deficits before the deposition of insoluble plaques. Levels of soluble Aβ are also a strong indicator of synaptic deficits and concurrent AD neuropathologies in post-mortem AD brain; however, it remains poorly understood how this soluble amyloid pool builds within the brain in the decades leading up to diagnosis, when a patient is likely most amenable to early therapeutic interventions. Indeed, characterizing early intracellular Aβ accumulation in humans has been hampered by the lack of Aβ-specific antibodies, variability in the quality of available human brain tissue and the limitations of conventional microscopy. We therefore sought to investigate the development of the intraneuronal Aβ pathology using extremely high-quality post-mortem brain material obtained from a cohort of non-demented subjects with short post-mortem intervals and processed by perfusion-fixation. Using well-characterized monoclonal antibodies, we demonstrate that the age-dependent intraneuronal accumulation of soluble Aβ is pervasive throughout the entorhinal cortex and hippocampus, and that this phase of the amyloid pathology becomes established within AD-vulnerable regions before the deposition of Aβ plaques and the formation of tau neurofibrillary tangles. We also show for the first time in post-mortem human brain that Aβ oligomers do in fact accumulate intraneuronally, before the formation of extracellular plaques. Finally, we validated the origin of the Aβ-immunopositive pool by resolving Aβ- and APP/CTF-immunoreactive sites using super resolution structured illumination microscopy. Together, these findings indicate that the lifelong accrual of intraneuronal Aβ may be a potential trigger for downstream AD-related pathogenic events in early disease stages.

Keywords Intraneuronal Aβ · Aβ oligomers · Tau pathology · Entorhinal cortex · Alzheimer's disease · Non-cognitively impaired

Introduction

The established neuropathological features of Alzheimer's disease (AD) include the presence of extracellular amyloid-β (Aβ) plaques and intracellular tau neurofibrillary tangles

Electronic supplementary material The online version of this article (https://doi.org/10.1007/s00401-018-1922-z) contains supplementary material, which is available to authorized users.

✉ A. Claudio Cuello
claudio.cuello@mcgill.ca

[1] Department of Neurology and Neurosurgery, McGill University, Montreal, QC, Canada

[2] Department of Pharmacology and Therapeutics, McGill University, Montreal, QC, Canada

[3] Human Brain Research Laboratory, Institute of Experimental Medicine, Hungarian Academy of Sciences, Budapest, Hungary

[4] Department of Psychiatry, Szent Borbála Hospital, Tatabánya, Hungary

[5] Laboratory of Cerebral Cortex Research, Institute of Experimental Medicine of the Hungarian Academy of Sciences, Budapest, Hungary

[6] Department of Anatomy and Cell Biology, McGill University, Montreal, QC, Canada

(NFT). The former is believed to be the result of a lifelong buildup of Aβ, whereby the continuous accumulation of soluble Aβ peptides leads to the spontaneous aggregation and formation of insoluble plaque deposits. It is thought that excessive accumulation of toxic Aβ material is the initiating component in a cascade of events leading to tau hyperphosphorylation, NFT formation and progressive cognitive decline, better known as the amyloid cascade hypothesis [30, 61]. This AD-neuropathological cascade is likely triggered well before the onset of clinical symptoms, evolving silently for decades while causing widespread neural damage [32, 61]. However, advanced Aβ plaque deposition is a poor correlate of AD-related cognitive decline and NFT density in AD-vulnerable brain regions [1, 17, 48, 58]. Although the widespread deposition of plaques is inarguably disease-associated, it is evident that this insoluble pool may not necessarily be the primary driver of cognitive dysfunction in AD.

Levels of soluble Aβ have proven to be a better predictor of synaptic dysfunction, cognitive impairment and concurrent neuropathologies when analyzed in post-mortem AD brain [2, 37, 46, 48]. Moreover, soluble Aβ oligomers have been shown to decrease cell survival and impair synaptic function in vitro [41, 56, 64, 75]. Reducing soluble Aβ levels by passive-immunization or genetic modulation of *APP* expression reverses synaptic deficits and cognitive impairments in several AD-animal models, even though established plaque pathology remains stable following treatment [19, 22, 66].

It was first demonstrated over two decades ago that neurons can generate intracellular Aβ peptides in vitro [65, 76, 79]. It has since been found that Aβ accumulates within neurons of AD-vulnerable regions before the formation of extracellular plaques, both in transgenic animal models of AD and post-mortem human brain, as reviewed in [11, 39]. Several transgenic models overexpressing mutated human *APP* or *PSEN* genes exhibit robust intraneuronal Aβ (iAβ) accumulation coincident with the onset of synaptic disruptions, LTP impairment and cognitive deficits in the absence of extracellular Aβ plaques [3, 7, 8, 10, 21, 31, 44, 45, 54, 56, 69, 80]. iAβ material has repeatedly been observed in post-mortem brains of patients with mild cognitive impairment (MCI) and AD, as well as cognitively unimpaired subjects [12–14, 24, 25, 40, 51], bringing into question the physiological and pathological significance of iAβ within the brain. It has also been shown that iAβ accumulation precedes extracellular plaque deposition in post-mortem brains of young Down's syndrome individuals [6, 28, 52], who express the *APP* gene in triplicate and exhibit increased production and aggregation of Aβ early in life [43, 55, 57].

Although the occurrence of iAβ has been reported across several brain regions and patient cohorts, findings from these studies have been disputed as a result of technical limitations and confounding factors [26]. For example, commercially available antibodies used to detect the cleaved Aβ peptide are unable to differentiate the same epitope located within the APP holoprotein or other cleavage products, including the C-terminal fragment (CTF) and sAPPα. Double-fluorescent immunolabeling of Aβ and APP is further hindered by the fact that widefield and confocal microscopy cannot adequately resolve discrete patterns of immunoreactivity that result in dense fluorescent signals. Inconsistent fixation methods, improper storage conditions and variable immunolabeling techniques may also explain conflicting reports on the occurrence of iAβ within the human brain. We have previously shown in a transgenic rat model that APP- and Aβ-immunoreactive sites represent distinct intracellular entities that can only be fully resolved by super resolution microscopy [31]; however, it remains poorly understood how the intracellular accumulation of soluble Aβ in humans contributes to the AD disease-continuum, most importantly, during preclinical stages of disease progression. Moreover, information on the presence of oligomeric iAβ in the non-AD brain is limited and contradictory, especially in cases with few or no Aβ plaques.

We therefore sought to investigate the occurrence of intracellular Aβ-immunoreactive (IR) material within the control human brain using extremely well-preserved post-mortem brain tissue and well-characterized monoclonal antibodies. We focused our investigation on the intraneuronal accumulation and oligomerization of soluble Aβ in relation to the development of insoluble Aβ and tau pathologies in the medial temporal lobe (MTL), a brain region which is vulnerable to early AD pathology. Analysis of brain material from non-demented subjects with minimal concurrent AD-related pathologies revealed that the accumulation of iAβ is ubiquitous and progressive, even in the absence of extracellular Aβ plaques and tau hyperphosphorylation.

Methods

Human tissue

Control human brain tissue samples were obtained from male and female subjects ($n = 12$) who died from causes not directly involving brain disease (Table 1). None of the subjects had a history of dementia or other neurological disorders. Information about subjects' level of education and cognitive status at the time of death was not available. Subjects were processed for autopsy in Saint Borbála Hospital, Department of Pathology, Tatabánya, Hungary. Informed consent was obtained for the use of brain tissue after death and for access to medical records for research purposes. Tissue was obtained and used in compliance with the 1964 Declaration of Helsinki and its amendments or comparable ethical standards, and all procedures were approved

Table 1 Demographic and medical information of case studies

Case	Subject identifier	Age	Sex	Post-mortem delay (h:m)	Cause of death
1	SKO2	74	M	4:55	Bronchopneumonia
2	SKO13	60	F	3:25	Respiratory arrest
3	SKO7	55	M	3:39	Pulmonary embolism with acute pulmonary heart disease
4	SKO14	66	M	3:25	Conduction disorder
8	SKO8	70	F	2:38	Myocardial infarction
6	SKO3	59	F	5:05	Cardiogenic shock
7	SKO17	75	F	4:35	Acute transmural myocardial infarction
8	SKO11	77	M	2:55	Cardiac arrest, cause unspecified
9	SKO5	77	F	4:04	Heart failure, unspecified
10	SKO18	85	M	2:52	Congestive heart failure
11	SKO16	72	M	2:22	Respiratory arrest
12	SKO10	83	M	4:03	Cardiac arrest, cause unspecified

List of cases. Case number, subject identifier, age in years, gender (*F* female, *M* male), post-mortem delay (h:min) and cause of death

by the Regional and Institutional Committee of Science and Research Ethics of Scientific Council of Health [EET TUKEB 31443/2011/EKU (518/PI/11)].

Brains were removed 2–5 h post-mortem, both the internal carotid and vertebral arteries were cannulated, and the brains were perfused first with physiological saline containing 0.33% heparin (1.5L in 30 min), followed by fixative solution containing 4% paraformaldehyde, 0.05% glutaraldehyde, and 0.2% picric acid in 0.1 M phosphate buffer (4-5L in 1.5-2 h). The MTL was dissected after perfusion and post-fixed in the same fixative solution overnight, but without glutaraldehyde [74]. Once received at McGill University, tissue blocks were frozen over liquid nitrogen and stored at − 80 °C before being cut into 40-µm-thick sections using a freezing microtome (Leica SM 2000R, Germany). Free-floating brain sections were stored in cryoprotectant solution (1.1 M sucrose, 37.5% ethylene glycol in phosphate buffer saline [PBS]) at − 20 °C until processed for immunohistochemistry (IHC).

Brightfield immunohistochemistry

Tissue sections were washed of cryoprotectant with PBS and subjected to heat-induced antigen retrieval (HIAR) by treatment with Tris–EDTA buffer (pH 9.0) for 30 min at 90 °C. After cooling for 20 min, endogenous peroxidase activity was quenched with 3% H_2O_2 and 10% methanol in PBS for 30 min at room temperature. Tissue sections were blocked with 0.1 M lysine and 10% normal goat serum (NGS) in PBS with 0.2% Triton X-100 (PBS-T) for 24 h at 4 °C to reduce non-specific antibody-binding. Immunolabeling was then performed using the following primary antibodies in 5% NGS in PBS-T overnight at 4 °C: anti-Aβ mouse monoclonal antibody, McSA1 (1:4000; Medimabs, Canada) [27]; anti-APP/CTF rabbit polyclonal antibody, pab27576 (1:1000; provided by Dr. Gerhard Multhaup, McGill University) [20, 31, 34]; anti-paired helical filament (PHF) mouse monoclonal antibody, NOAL (1:10; provided by Dr. Michal Novak, Slovak Academy of Science) [49, 81]. Aβ oligomers were detected using the well-characterized mouse monoclonal antibody, NU1 (1:500; provided by Dr. William Klein, Northwestern University) [42], in sections that were not subjected to HIAR before immunolabeling. Phosphorylated tau was detected using anti-phospho-tau (Ser^{202} and Thr^{205}) mouse monoclonal antibody, AT8 (1:2000; Thermo Fisher Scientific, USA), for 40 h at 4 °C, as described by Braak et al. [4]. To verify antibody specificity, McSA1 and pab27576 antibodies were incubated with 5ug of human $Aβ_{1-42}$, $Aβ_{1-16}$ or $Aβ_{17-42}$ peptide (rPeptide, USA) for 1 h at room temperature with head-over-tail shaking before performing IHC. Tissue sections were then incubated with the following secondary antibodies: goat anti-mouse-IgG (1:100; MB Biochemicals, Canada), biotinylated goat anti-rabbit-IgG (1:200; Vector Laboratories, USA), and bi-specific monoclonal antibody, MCC10 [36, 50, 62], pre-incubated with 5 ug/mL horseradish peroxidase (HRP). Control experiments performed in the absence of primary antibodies showed no cross-reactivity of secondary antibodies. Signal amplification was performed with either mouse anti-HRP monoclonal antibody (1:30) pre-incubated with 5 µg/mL HRP (MAP kit, MediMabs, Canada) or Vectastain ABC-HRP kit (Vector Laboratories, USA). Stainings were developed with 0.06% 3,3′-diaminobenzidine as a chromogen and 1% H_2O_2. Sections were mounted on gelatin-coated slides, dehydrated with a graded ethanol series, delipidated in xylene and cover-slipped with Entellan (MilliporeSigma, USA). Images were acquired using an Axio Imager M2

microscope equipped with an AxioCam 506 color digital camera (Carl Zeiss, Germany).

Quantification of AD-related pathologies in the EC

Relative intensity of neuronal McSA1-IR

To quantify and compare levels of iAβ between subjects, we used a highly specific monoclonal antibody, McSA1, which targets the N-terminal amino acids 1–12 of human Aβ. Following IHC, we performed a semi-quantitative analysis measuring the relative intensity of neuronal McSA1-IR. Images focused on layer II of the EC were acquired using a 20× objective, converted to 8-bit and variably thresholded using ImageJ software (National Institutes of Health, USA) so neurons could be precisely delineated and manually selected as regions of interest (ROI) using the 'Analyze Particles' function. The integrated density and area of each ROI (i.e., each McSA1-IR neuron) were measured and summated (Σ integrated density/Σ area) to produce one value representing the total signal intensity for each image (y). Chromogen intensity was quantified using the reciprocal intensity (r) method [53]. Briefly, the relative "darkness" of each image is calculated using $r = 255 - y$, where 255 is the maximum intensity of unstained or "white" areas, and 'y' is the staining intensity of the ROIs being considered. As a result, higher 'r' values are associated with more intense chromogen staining. All tissue sections were processed simultaneously to maintain identical immunolabeling and staining conditions.

Surface area of McSA1-IR Aβ plaques and AT8-IR neuropil threads and cells

Using McSA1 to immunolabel Aβ plaques, images acquired using a 10x objective were again converted to 8-bit and variably thresholded to delineate plaque deposits within the EC (Fig. 1). The total surface area occupied by Aβ plaques across all layers of the EC was measured using the 'Analyze Particles' function and expressed in mm^2. A similar analysis was performed within the same region by measuring the surface area occupied by AT8-IR neuropil threads and cells; this value was normalized according to the size of the region measured and expressed in mm^2.

Fluorescent immunohistochemistry

Tissue sections were subjected to HIAR as described above, permeabilized with 50% ethanol and blocked overnight with 0.1 M lysine in 10% NGS. Double-immunolabeling was performed using McSA1 (1:250) and pab27576 (1:500) primary antibodies in 5% NGS overnight at 4 °C, followed by incubation with Alexa Fluor 488 goat anti-mouse and Alexa Fluor 568 goat anti-rabbit antibodies (1:400; Life Technologies, USA) for 2 h at room temperature. To abolish tissue auto-fluorescence associated with lipofuscin, sections were incubated with 0.3% Sudan Black in 70% ethanol for 15 min at room temperature with fast shaking. Finally, sections were counterstained with 4′,6-diamidino-2-phenylindole (DAPI) for 3 min at room temperature before being mounted and cover-slipped with Aqua Polymount (Polysciences Inc., USA). Images were acquired using a super resolution DeltaVision OMX V4 Blaze system (Applied Precision, GE Healthcare, UK).

Structured illumination microscopy and colocalization analysis

To resolve McSA1 and pab27576 fluorescent-IR sites, we employed super resolution SIM. Three tissue sections per subject ($n = 6$) were immunolabeled as described. For each tissue section, 5–8 images centered on 1–2 neuronal cell

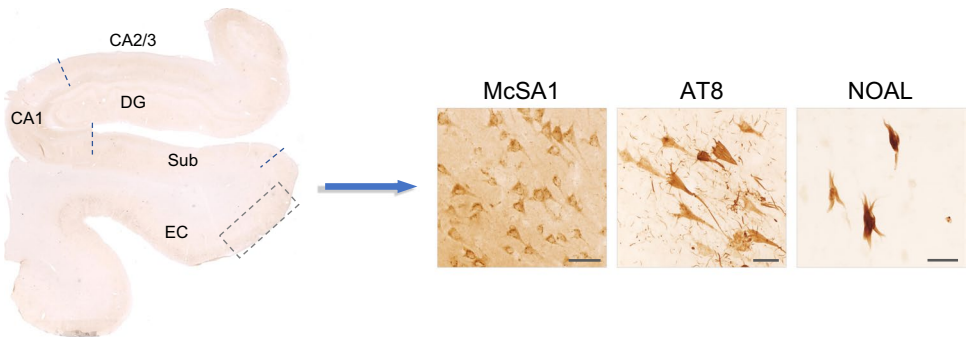

Fig. 1 Quantifying AD-related pathologies within the medial temporal lobe of non-demented cases. 40 µm-thick tissue sections comprising the EC, subiculum (Sub), CA regions, and dentate gyrus (DG) were subjected to HIAR and IHC. To quantify the extent and severity of Aβ and tau pathologies, Aβ was probed using McSA1; phospho-tau (Ser^{202} and Thr^{205}) was probed using AT8; and tau PHF were probed using NOAL. Images from comparable regions of the EC (denoted above) were acquired by brightfield microscopy and quantified by ImageJ software. Unless otherwise specified, quantification was performed across all cell layers of the EC (scale bar = 50um)

bodies were acquired in the EC and CA1 using a 100× objective lens. To adequately capture the depth of the cell nucleus and cytoplasm, 3-µm z-stacks were generated using the following channel settings: mode, EMCCD 5 MHz; EMCCD Gain, 170; Exposure, 10 ms; Percent transmission for lasers 405, 31.3%; 488, 1.0%; 568, 10.0%. To measure the extent of colocalization between McSA1- and pab27576-IR areas, Pearson and Manders' correlation coefficients were calculated using the JACop plugin in ImageJ software. The Pearson coefficient describes the linear relationship between fluorescent signals and varies between 1 and -1. Manders' M1 and M2 coefficients represent the fraction of colocalized fluorescent signals, where 0 is defined as no colocalization and 1 is defined as perfect colocalization. To offset background fluorescence inherent to human brain tissue, images acquired within the EC and CA1 were set at a threshold of 16/12 and 16/16, respectively, for McSA1/pab27576 channels prior to colocalization analysis. Using the Volocity 3D image Analysis Software (PerkinElmer, USA), serial *z*-planes were also reconstructed and assembled to form a representative 3D model.

Results

Whole-tissue perfusion of post-mortem human brain material

The ability to reliably detect proteins in post-mortem human brain tissue by IHC is largely dependent on the quality of the material being used. Therefore, to study the occurrence of iAβ within the human brain, we used well-preserved post-mortem brain tissue from non-demented subjects who died of causes unrelated to neurological disease (Table 1). Tissue harvest was performed on samples with an average post-mortem delay of 3.65 h (ranging between 2 and 5 h for all cases), thus limiting possible tissue damage and protein degradation. Perfusion via the carotid and vertebral arteries, a technique not commonly used, ensured that all contents of the brain's vasculature were eliminated and that a continuous flow of fixative solution was applied to achieve complete, rapid and even tissue fixation. For this study, we used material from the MTL and adjacent areas comprising the complete circuitry of the entorhinal cortex (EC), subiculum, cornu ammonis (CA) regions, and dentate gyrus (DG). Using tissue sections from these samples, we investigated the accumulation of Aβ and phosphorylated tau by IHC, which are classical molecular hallmarks of AD-related pathologies, as illustrated in Fig. 1.

Soluble iAβ accumulation is predominant in the EC compared with insoluble Aβ plaque and tau pathologies

To characterize the neuronal accumulation of soluble Aβ in relation to the development of insoluble Aβ and tau pathologies, we performed quantitative analyses of McSA1, AT8 and NOAL immunolabeling within the EC (Fig. 1), a brain region regarded as 'ground-zero' for NFT formation and subsequent spread of tauopathy in the MTL [4, 5].

First, we used a well-characterized monoclonal antibody, McSA1, to detect Aβ-burdened neurons in layers II–VI of the EC. All neurons in this region were immunopositive for McSA1 across all subjects (Fig. 2; Supplemental Fig. 1). Cell-number quantification revealed an average of 3030 Aβ-burdened neurons per 10 mm^2 of tissue analyzed (Table 2).

In only two cases, it was not possible to definitively quantify the number of McSA1-IR neurons. In subject SKO2, the contrast between intraneuronal and extraneuronal immunostaining was too low to accurately identify immunopositive cells in entorhinal layers III and V. Additionally, extensive plaque pathology in subject SKO10 occluded the accurate quantification of neurons in entorhinal layers II–VI, although neurons could still be clearly visualized in plaque-free areas and exhibited intense McSA1-IR (Supplemental Fig. 1).

iAβ was also observed in the MTL of one subject diagnosed with AD (76 years old; Supplementary Fig. 1). This is consistent with previous studies that have demonstrated the occurrence of iAβ within the AD brain. Neuronal McSA1-IR was found throughout all regions of the MTL, although Aβ-burdened neurons within the EC were notably sparse due to the presence of advanced plaque pathology, as well as frank neuronal loss and degeneration.

We then measured the intensity of neuronal McSA1-IR in layer II of the EC using the reciprocal intensity (*r*) method, and subjects were classified in increasing order of iAβ-burden (Fig. 2; Table 2). Layer II neurons were consistently and clearly visualized in nearly all cases.

Next, we quantified the extent and severity of insoluble Aβ and tau pathologies across all layers of the EC to assess the possible development of concurrent AD-related pathologies in these non-demented cases. Four subjects exhibited limited plaque pathology that was restricted to the EC (Table 2). As described, case SKO10 displayed more advanced plaque deposition, which extended to most regions of the MTL. The remaining seven subjects did not exhibit any Aβ plaques within the EC or hippocampus.

We also quantified established tau pathology by measuring the surface area occupied by AT8-IR (Table 2). In most subjects, AT8-IR neuropil threads (NT) and NFT were observed only within the EC (Fig. 2), with few AT8-IR

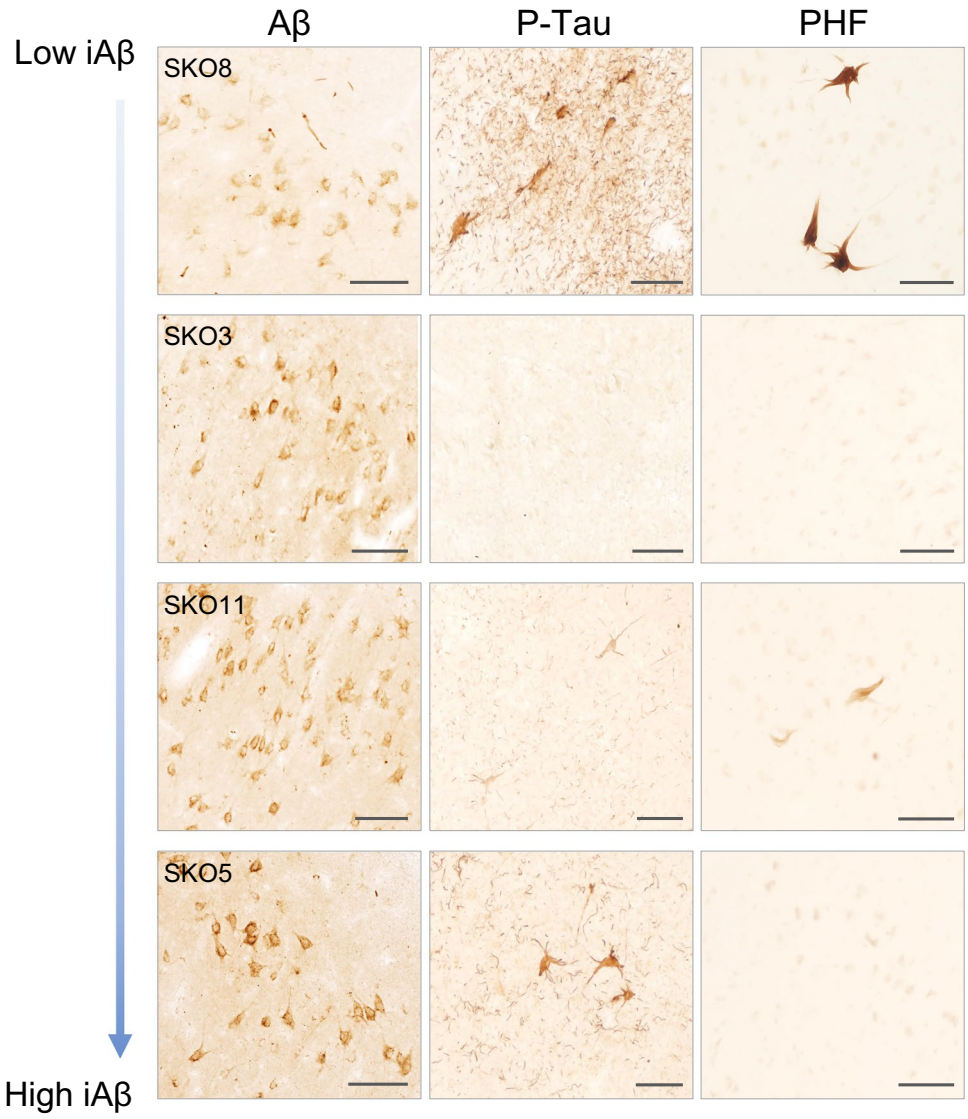

Fig. 2 Neuronal accumulation of Aβ material occurs in all subjects, independent of insoluble Aβ and tau pathologies. To evaluate the accumulation of iAβ in the EC with respect to concurrent insoluble pathologies, iAβ and extracellular plaques were detected using McSA1; phospho-tau, NT and NFT were detected using AT8; and tau PHF were detected using NOAL (scale bar = 100 µm). Subjects are arranged in order of increasing iAβ burden in layer II, as described in Table 2

neurons found in regions extending beyond CA1. Two subjects were completely devoid of AT8 immunolabeling within the EC (SKO3 and 16). Additionally, only one case exhibited more extensive tau pathology characterized by the presence of NT and NFT in the subiculum and all CA regions (SKO7).

Lastly, to reveal more advanced pathological tau structures, we used a rat monoclonal antibody, NOAL, raised against pronase-resistant tau PHF [49, 81]. Only four subjects exhibited immunopositive cell bodies containing stable PHF, which were relatively sparse and limited to layer II of the EC (Fig. 2; Table 2).

Overall, we found that the neuronal accumulation of Aβ-IR material was significantly more pervasive than insoluble Aβ and tau pathologies. McSA1-IR neurons within the EC far-outnumbered those immunolabeled with AT8 or NOAL, and all 12 subjects exhibited detectable levels of neuronal McSA1-IR, independent of other AD-related pathologies (Table 2; Fig. 2). Importantly, two subjects exhibited significant iAβ accumulation and few Aβ plaques in the absence of detectable AT8-IR in the EC (SKO3 and 16). Conversely, three subjects exhibited strong neuronal McSA1-IR while devoid of Aβ plaques and with minimal AT8-IR in the same region (SKO13, 14 and 11). Additionally, the relative intensity of neuronal McSA1-IR did not appear to correlate with Aβ plaque-load, tau AT8-IR or PHF (Table 2). These results suggest that the neuronal accumulation of soluble Aβ likely precedes both Aβ plaque and tau tangle formation in the EC.

iAβ accumulation increases as a function of age in the EC

Although the presence of iAβ within the EC was ubiquitous across all subjects, independent of concurrent Aβ plaque and tau pathologies, we observed significant variability in

Table 2 Assessment of AD-related neuropathologies in the non-demented entorhinal cortex

Case	Subject identifier	McSA1-IR neurons[a]	Intensity of intracellular Aβ-IR[b]	Extracellular Aβ plaques[c]	AT8-IR[d]	AT8-IR neurons[a]	PHF[a]
1	SKO2	*	119.209	–	0.126	53.0	46.1
2	SKO13	2944.0	124.991	–	0.015	3.7	–
3	SKO7	2873.6	126.714	–	0.113	92.3	–
4	SKO14	3538.1	128.664	–	0.010	15.3	–
8	SKO8	2873.6	129.014	0.249	0.165	36.6	9.8
6	SKO3	3409.1	133.549	0.167	–	–	–
7	SKO17	3158.5	136.733	–	0.028	5.74	–
8	SKO11	3005.2	138.519	–	0.012	12.6	2.2
9	SKO5	3354.0	139.345	–	0.102	12.9	–
10	SKO18	2764.5	140.468	0.003	0.117	29.3	11.0
11	SKO16	2943.3	144.931	0.040	–	–	–
12	SKO10	*	*	2.405	0.289	55.3	–

*Diminished and erratic intraneuronal IR across entorhinal layers

[a]Number of McSA1-IR neurons, AT8-IR neurons and NOAL-IR paired-helical filaments (PHF) across layers II–VI, expressed per 10mm^2

[b]Intensity of intraneuronal McSA1-IR in layer II, expressed as the reciprocal integrated density/area (r)

[c]Total surface area occupied by extracellular Aβ plaques (mm^2) across layers II–VI

[d]Surface area occupied by AT8-IR across layers II–VI, expressed per 10mm^2 (mm^2)

the intensity of neuronal McSA1-IR between cases. Interestingly, we noticed that neurons within the EC exhibited stronger immunostaining and tended to be more clearly defined in older subjects compared with younger subjects across all entorhinal layers (Fig. 3a). Additionally, three cases with the most advanced age at death exhibited higher levels of iAβ compared with three cases with the least advanced age (Fig. 3b). To validate this observation, we performed a linear regression analysis assessing the relationship between subject-age and neuronal McSA1-IR (r) in layer II of the EC ($n=10$), as described in Table 2. Statistical analysis revealed an R^2 value of 0.379 that was just below the threshold of statistical significance ($p=0.058$), suggesting that iAβ accumulation increases with age in this patient cohort (Fig. 3c). Two subjects were excluded from the analysis due to advanced plaque deposition coinciding with erratic immunolabeling in the region analyzed (SKO2 and 10; Table 2). These results suggest that the progressive, lifelong buildup of iAβ may contribute to the pathogenic mechanisms that confer age as a risk factor for the development of AD.

iAβ is pronounced in AD-vulnerable regions, but is largely absent within the cerebellum

Similar to what was observed in the EC, we found that neurons within the subiculum, CA regions, and DG exhibited significant accumulation of iAβ material (Fig. 4a). In general, the intensity of neuronal McSA1-IR in the hippocampus paralleled that observed in the EC: those subjects with higher levels of iAβ in the EC exhibited higher neuronal McSA1-IR in other regions of the MTL. Of the cases without extracellular plaque deposition, one subject was devoid of AT8-IR within the hippocampus (SKO3), while three additional cases presented with few sparse AT8-IR neurons in the absence of NT (SKO13, 14 and 5). Given that iAβ could consistently be visualized in this cohort of non-demented cases, even in the absence of Aβ plaque and tau pathologies, our results suggest that the neuronal accumulation of soluble Aβ may precede the development of insoluble AD-related pathologies within the hippocampus. In addition, the fact that McSA1-IR could be detected in all neurons of the MTL indicates that the intracellular accumulation of Aβ may be a characteristic of neurons within AD-vulnerable regions.

To investigate the occurrence of iAβ in brain regions differentially affected by AD pathology, we probed tissue sections from the cerebellum of these same cases by IHC. In this region, Aβ plaque deposition and tissue atrophy are typically only observed at very late disease stages without NFT formation or tauopathy [71, 78]. We therefore analyzed the cerebellar grey matter of four non-demented cases to evaluate the occurrence of iAβ accumulation in cerebellar neurons. McSA1-IR within this region was relatively homogenous and cell bodies could not be distinguished from the surrounding neuropil (Fig. 4b). Aβ-immunoreactive neurons were detected in only one case: these neurons were faintly immunostained and were identified as small granule neurons (Fig. 4b). Interestingly, we noted that this unique case corresponded to one

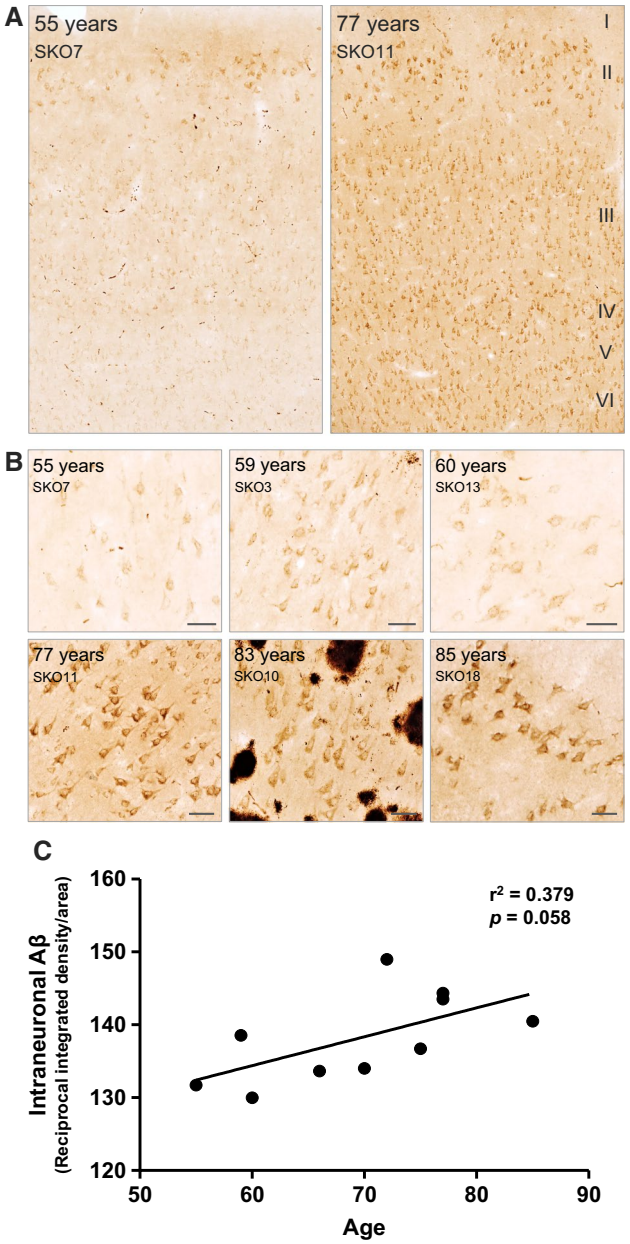

Fig. 3 Neuronal McSA1-IR increases with age in the EC. **a** McSA1-IR neurons exhibited more intense chromogen staining across all layers of the EC in older subjects compared with younger subjects. Entorhinal layers are denoted above. **b** Three subjects with the oldest age at death exhibited significantly more neuronal McSA1-IR within the EC (bottom panels) compared with three subjects with the youngest age at death (top panels) (scale bar = 50 µm). **c** Linear regression analysis suggested that the intensity of neuronal McSA1-IR is related to subject-age within this patient cohort ($n = 10$; $y = 110.598 + 0.397x$; $R^2 = 0.379$; $p = 0.058$)

of the oldest subjects within our cohort (77 years, SKO11). This case also exhibited objectively lower levels of iAβ within the cerebellum compared with the MTL (Fig. 2). Our findings suggest that brain regions affected in early disease stages exhibit higher levels of iAβ compared with regions that are less-susceptible to such neurodegenerative processes.

Advanced plaque deposition mirrors the anatomical distribution of Aβ-burdened neurons

While assessing the relationship between soluble iAβ accumulation and insoluble AD-related pathologies in the MTL, we noticed a striking similarity between the localization of extracellular plaque deposition in one case with advanced plaque pathology (83 years, SKO10) and the anatomy of Aβ-burdened neurons (Fig. 5). We found that lake-like Aβ deposits in the presubiculum exhibited a spatial geometry that overlapped almost perfectly with the anatomical distribution of discrete islands of McSA1-IR parvopyramidal neurons in subjects devoid of Aβ plaques. These lake-like Aβ aggregates, originally described by Kalus et al. and others [35, 72, 82], exhibited sharp, triangular delineations occurring at regular spatial intervals.

In contrast with the presubiculum, a pattern of Aβ plaque deposition in the EC presented as a negative image with islands of Aβ-burdened neurons in subjects without plaque pathology: a 'clean' band in layer II was devoid of extracellular plaques, as well as McSA1-IR neurons. Plaque deposits in layer I formed small but clear protrusions into layer II at regular intervals, reminiscent of the negative space formed between distinct islands of Aβ-burdened layer II neurons.

These observations raise questions regarding the origin of extracellular plaques and the dynamics between intraneuronal and extraneuronal Aβ. In this regard, high levels of iAβ in AD-vulnerable brain regions may contribute to the distinct spatial and sequential pattern of plaque deposition previously reported within post-mortem non-demented and AD brain.

Aβ oligomers accumulate intraneuronally within the non-demented human brain

It is well-documented that Aβ oligomers are likely the most toxic amyloid species within the human brain; however, the occurrence of oligomeric iAβ within the control MTL in the absence of Aβ plaques remains poorly understood. Given the quality of the tissue used in this study, we decided to assess the anatomical and cellular distribution of soluble Aβ oligomers within the non-demented MTL by IHC using NU1, a well-characterized conformation-specific monoclonal antibody that targets Aβ oligomers with minimal reactivity to monomers [42]. Unlike McSA1, which exhibited strong neuronal-IR in all regions of the MTL, NU1 immunolabeling was most prominent in CA3 neurons located within the boundaries of the polymorphic layer of the DG (Fig. 6). All cases presented with evident neuronal immunolabeling, with the exception of one case (72 years, SKO16). Although the

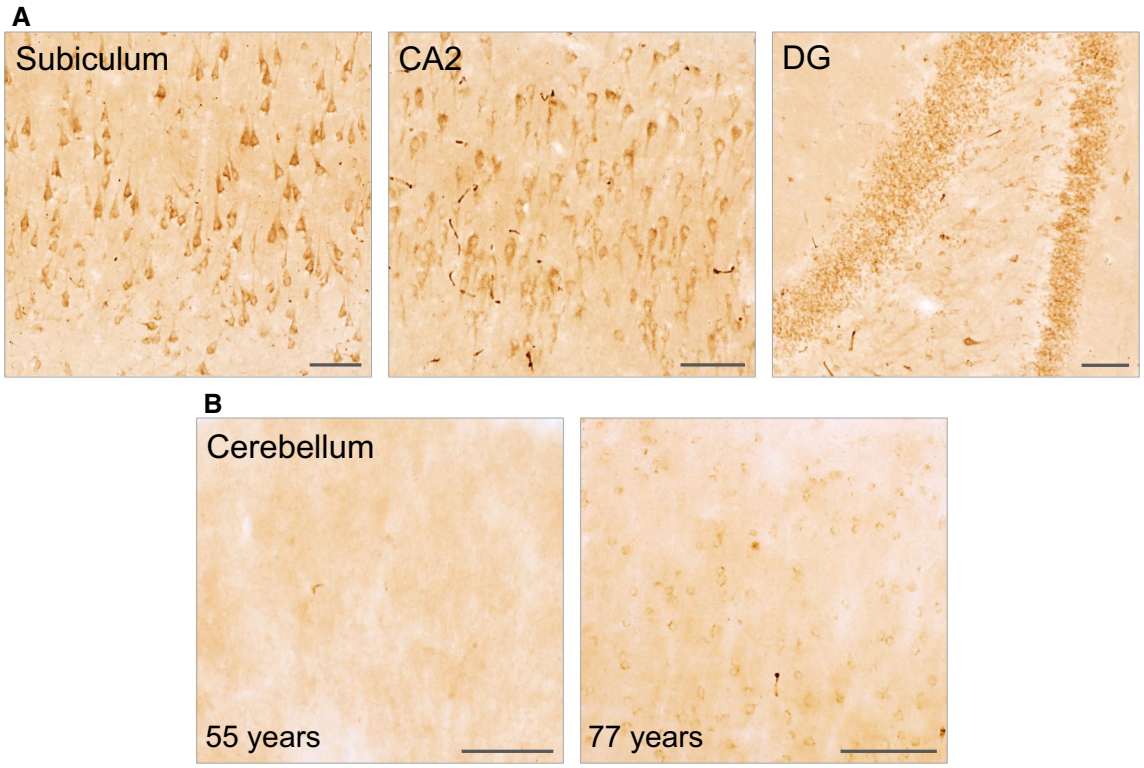

Fig. 4 Age-dependent iAβ accumulation is more prominent in the MTL compared with the cerebellum. **a** Neuronal McSA1-IR was observed in all regions of the MTL, including the subiculum, CA regions, and DG. Anatomical boundaries could be delineated from neuronal McSA1-IR alone (scale bar = 100 µm). **b** McSA1 did not show neuron-specific immunolabeling in the cerebellum of most cases analyzed; in these subjects, immunolabeling within the cerebellar grey matter was relatively homogenous (left panel). In one of the oldest cases, faint immunolabeling of granule cells was visualized (right panel) (scale bar = 100 µm)

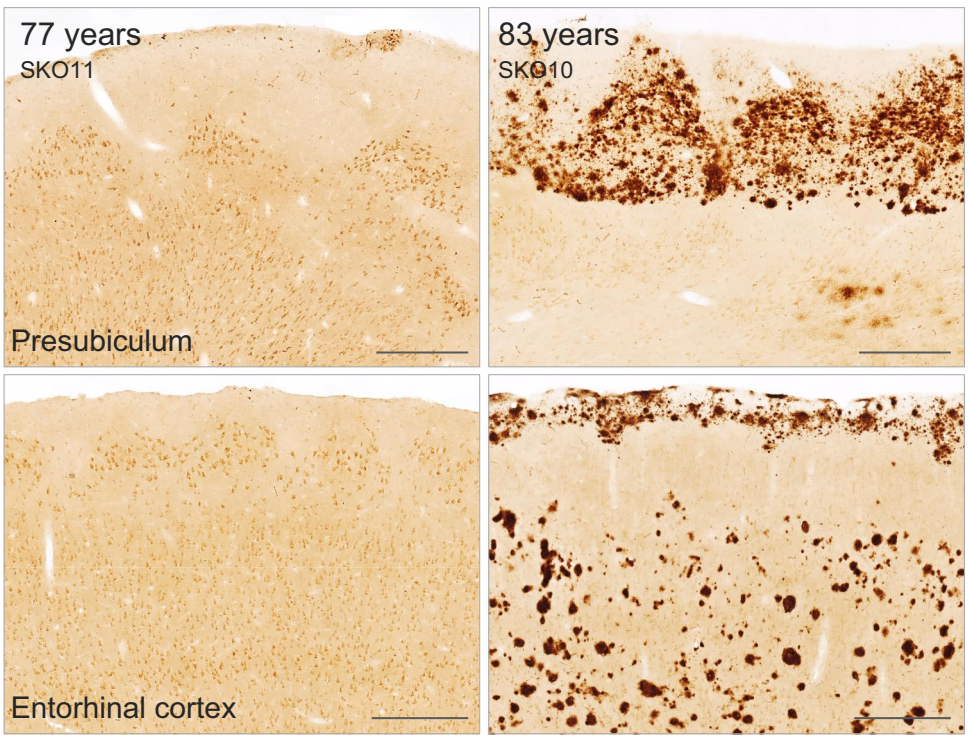

Fig. 5 Advanced Aβ plaque deposition mirrors the anatomical distribution of Aβ-burdened neurons. Within the presubiculum of one case with relatively advanced plaque pathology (top right panel), 'lake-like' amyloid deposits occurred in a distinct triangular pattern, similar to the anatomical arrangement of parvopyramidal Aβ-burdened neurons (top left panel). In contrast, subpial band-like plaque deposits in layer I and layer III of the EC (bottom right panel) formed a negative image with layer II Aβ-burdened neurons (bottom left panel) (scale bar = 500 µm)

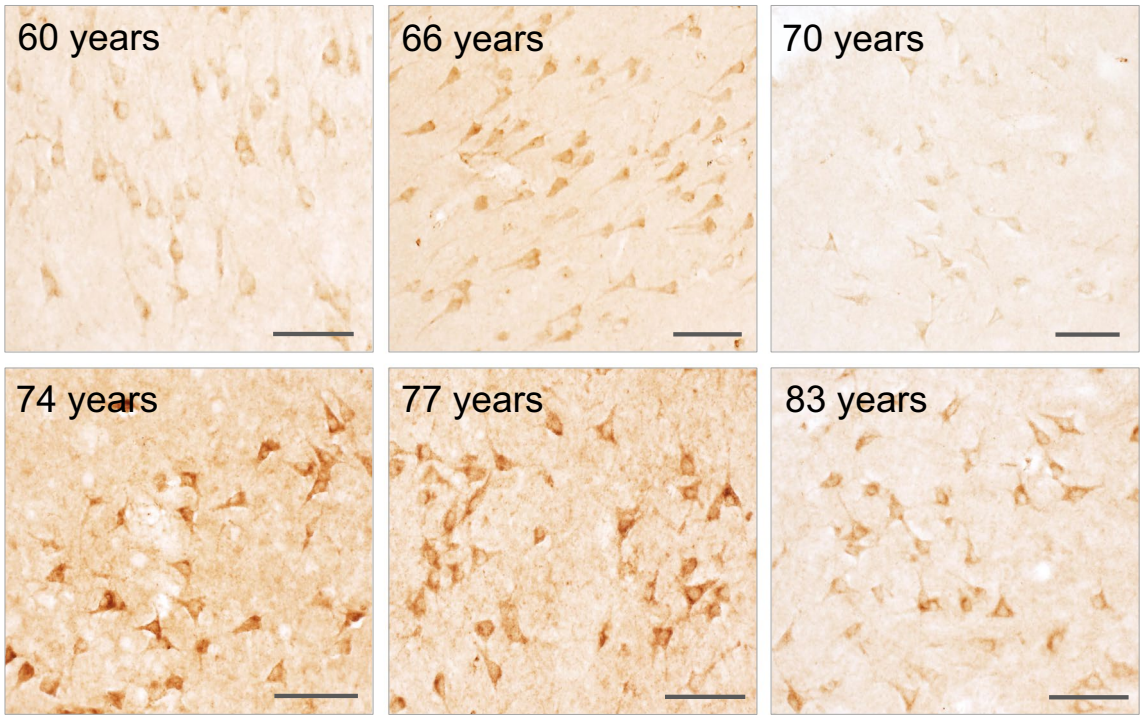

Fig. 6 Hippocampal neurons exhibit intracellular accumulation of Aβ oligomers. iAβ oligomers were probed using the conformation-specific monoclonal antibody, NU1. CA3 neurons located within the boundaries of the polymorphic layer of the DG exhibited strong neuronal immunolabeling across most subjects, regardless of plaque or tau pathologies (scale bar = 100 μm)

relative intensity of neuronal NU1-IR appeared highly variable across subjects, immunolabeling occurred independently of insoluble Aβ and tau pathologies, as well as neuronal McSA1-IR. The relative abundance of oligomeric iAβ was also unrelated to subject age or post-mortem delay. Variable neuronal immunolabeling was also observed within the transentorhinal cortex, subiculum and CA1. Interestingly, neuronal NU1-immunolabeling could only be observed in tissue not subjected to antigen retrieval. It is likely that conditions used for HIAR disrupt the intramolecular interactions of the Aβ oligomeric complex, rendering it unrecognizable by the conformation-specific NU1 antibody. These results suggest that the intracellular accumulation of Aβ oligomers may represent another mechanism by which Aβ disrupts neuronal function at early disease stages.

Neuronal Aβ and APP are distinct intracellular entities within the human brain

McSA1 immunolabeling revealed the presence of iAβ material in AD-vulnerable brain regions with and without insoluble AD-related pathologies. To verify that this intracellular IR pool is in fact associated with the Aβ peptide, as opposed to the APP holoprotein or cleavage fragments, we performed double-immunolabeling using McSA1 and the APP/CTF-specific polyclonal antibody, pab27576, which targets the C-terminal 43 amino acids of human APP, but does not recognize the Aβ domain.

The amino acid residues recognized by McSA1 are also located within APP and other cleavage products. We have previously shown by competition assay that McSA1 does not show specificity for full-length APP or sAPPα [27, 44]. To validate the specificity of both McSA1 and pab27576 antibodies in human tissue, we performed peptide pre-adsorption using human $A\beta_{1\text{-}42}$ peptide. Consistent with previous experiments, McSA1 immunolabeling was abolished by $A\beta_{1\text{–}42}$ pre-adsorption, while that of pab27576 was unaltered (Fig. 7a). We also performed pre-adsorption using human $A\beta_{17\text{–}42}$ and $A\beta_{1\text{–}16}$ peptide fragments to confirm the N-terminal binding site of the McSA1 antibody. Incubation with $A\beta_{17\text{–}42}$ peptide fragment did not interfere with McSA1 binding in tissue, while $A\beta_{1\text{–}16}$ fully sequestered the antibody in solution, preventing subsequent immunolabeling (Fig. 7b).

Next, to evaluate the extent of colocalization between McSA1- and pab27576-IR, we performed super-resolution SIM and quantitative colocalization analysis (Fig. 8a, b). In contrast with standard confocal microscopy, SIM can achieve a resolution of up to 100 nm in *x, y* and 250 nm in *z* [60] and can resolve distinct IR puncta. By calculating Pearson and Manders' coefficients, we found minimal colocalization between neuronal McSA1- and pab27576-IR within the EC (Fig. 8c). We determined that only 6.4% of

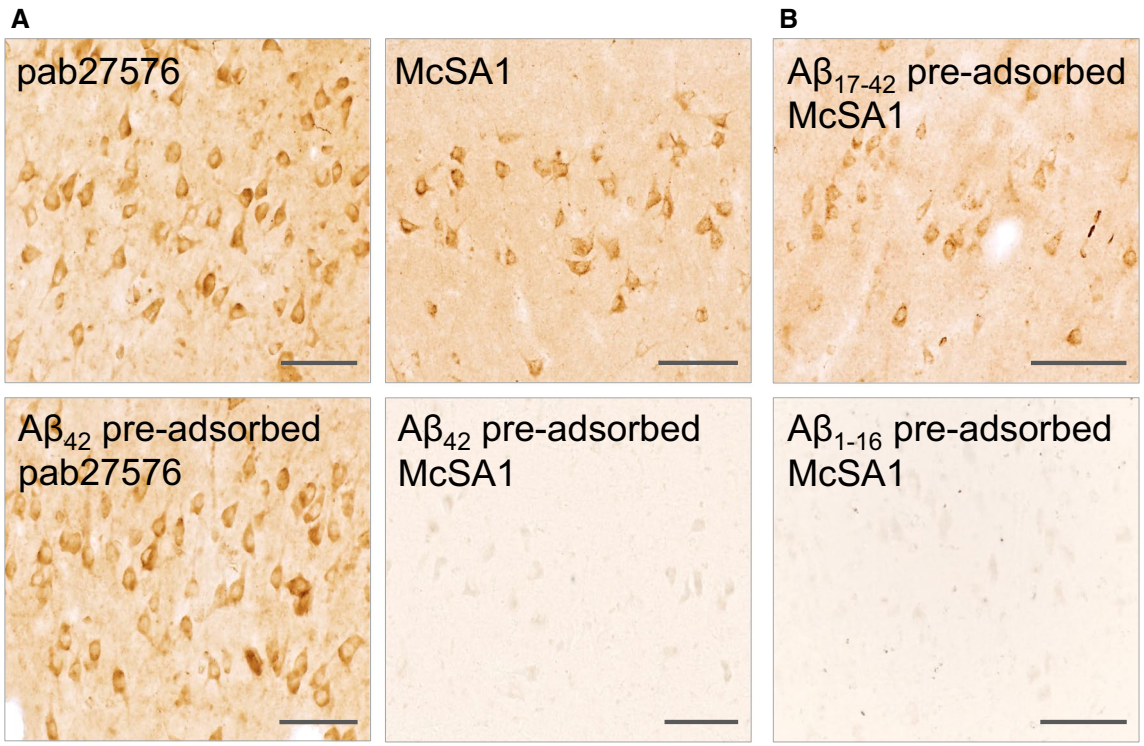

Fig. 7 Validating McSA1 and pab27576 antibody specificity by peptide pre-adsorption. **a** Antibody pre-adsorption using 5ug of human $A\beta_{1-42}$ completely abolished McSA1 immunolabeling (right panels), while pab27576-IR was largely unaffected (scale bar = 100 µm). **b** McSA1 binding in tissue was unaltered by pre-incubation with human $A\beta_{17-42}$, while human $A\beta_{1-16}$ peptide fragment containing the Aβ N-terminal epitope sequestered McSA1 in solution, preventing any observable IR (bottom panel) (scale bar = 100 µm)

McSA1-IR regions overlapped with that of pab27576 in this brain region ($M1 = 0.064 \pm 0.005$). Quantitative analysis of images acquired in CA1 similarly showed minimal colocalization between neuronal McSA1- and pab27576-IR.

Based on the pattern of McSA1-IR, we found that Aβ was evenly distributed throughout the neuronal cytoplasm, soma and dendrites, but was largely excluded from the cell nucleus. In contrast, pab27576-IR structures were notably denser and exhibited both cytoplasmic and nuclear localization in neurons, as well as neighboring glia. Given the clear differences in localization and intracellular distribution between McSA1 and pab27576, we concluded that both antibodies do in fact target distinct amyloid fragments within the neuronal space.

Discussion

Despite numerous investigations into the occurrence of iAβ within the human brain, reports on the neuronal accumulation of soluble Aβ have been repeatedly challenged and overshadowed by the prevailing view that insoluble plaques represent the dominant pathogenic agent within the AD brain. Lack of consensus on the relevance of intracellular Aβ in the context of AD has curtailed discussions on the potential biological and toxic effects of iAβ within the brain, particularly during early disease stages. Using well-characterized monoclonal antibodies, as well as extremely well-preserved human brain tissue from non-demented individuals with minimal AD-related pathologies, we demonstrate that Aβ is undoubtedly present within the intraneuronal space across several regions of the hippocampus and, most importantly, the EC, an area considered the epicenter of tau NFT propagation. Moreover, we provide evidence that iAβ is invariably present in all subjects analyzed, independently of concurrent insoluble Aβ and tau pathologies. We propose that the neuronal accumulation of soluble Aβ likely precedes the deposition of extracellular Aβ plaques, tau hyperphosphorylation, and the formation of tau NFT and PHF, given that intracellular Aβ-IR material was clearly observed in cases without such pathologies. Two subjects devoid of hyperphosphorylated tau within the EC displayed significant iAβ accumulation, even in the presence of only few plaque deposits. Similarly, three subjects without Aβ plaque pathology demonstrated substantial iAβ material with only minimal AT8-IR. Our results suggest that Aβ buildup within the EC does in fact precede the development of other classical disease hallmarks, but develops first as a soluble intraneuronal pool.

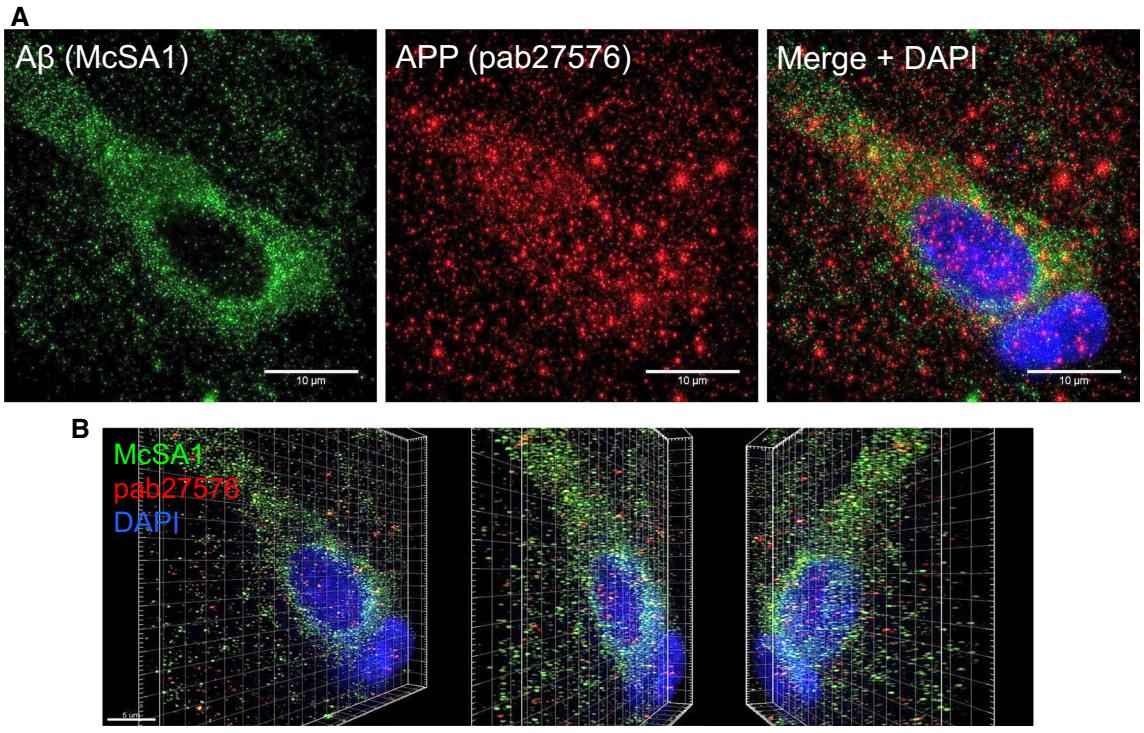

C

Co-localization analysis of McSA1- and pab27576-IR

Region	#Images	Pearson	Manders M1	Manders M2
Entorhinal Cortex	83	0.16 ± 0.005	0.064 ± 0.005	0.134 ± 0.007
CA1	78	0.18 ± 0.005	0.069 ± 0.005	0.095 ± 0.005

Manders M1: fraction of of McSA1-IR (green) co-localized with pab27576 (red)
Manders M2: fraction of pab27576-IR (red) co-localized with McSA1 (green)

Fig. 8 Sub-cellular distribution of neuronal McSA1-IR and colocalization with pab27576-IR. Intraneuronal Aβ and APP were immunolabeled using McSA1 (green) and pab27576 (red) antibodies, respectively. Neurons were identifiable based on their characteristic nuclear size and shape, as revealed by DAPI. **a** Images centered on neuronal cell bodies in the EC and CA1 underwent structured illumination reconstruction to resolve distinct IR puncta. **b** *Z*-stack projections were subjected to 3D reconstruction to better-illustrate the extent of colocalization between McSA1- and pab27576-IR sites within the neuronal space. **c** Quantitative colocalization analysis revealed that McSA1 and pab275762 occupy distinct regions of the intraneuronal space. Less than 7% of McSA1-IR overlapped with pab27576, as represented by a Manders M1 coefficient of 0.064 and 0.069 within the EC and CA1, respectively. A similarly small fraction of pab27576-IR colocalized with McSA1, as revealed by Manders M2 coefficients of 0.134 and 0.095 in the EC and CA1, respectively

Most interestingly, the quantity of iAβ material appeared to increase as a function of age in this non-demented cohort. This observation is consistent with previous studies that have reported an age-dependent increase in the accumulation of iAβ across a broad age-range of subjects (e.g., between 3 months and 79 years old) [25]. We performed a semi-quantitative analysis confirming this same phenomenon in a more comparable cohort of adults that spanned a narrower age-range (i.e., between 55 and 85 years old), which also more closely represents the stage in life at which people are most likely to develop cognitive deficits due to AD. Although the results of the analysis fell just below the threshold of statistical significance, it was striking that such a strong trend could still be observed in this relatively small cohort. The spontaneous, lifelong generation and accumulation of Aβ has long been implicated in the AD pathogenesis, whereby increasing brain-Aβ likely triggers the AD pathological cascade once is surpasses a homeostatic threshold [30, 61]. Importantly, we have shown in this study that the age-dependent increase in soluble Aβ also occurs within neurons of the MTL, the effects of which have been scarcely studied within the non-demented human brain. We know from transgenic animal models that early iAβ accumulation in the absence of extracellular plaques is sufficient

to produce synaptic deficits [69], LTP impairment [10, 54, 56], inflammation [20, 29, 33], oxidative stress [18, 47] and cognitive dysfunction [3, 21, 31, 44]. It is conceivable, therefore, that the lifelong buildup of iAβ material within the human brain may trigger these same mechanisms, instigating tau hyperphosphorylation and contributing to subsequent cognitive decline.

In most cases analyzed, neuronal McSA1-IR was completely absent in the cerebellar grey matter. iAβ was observed in granule neurons of only one subject, although the intensity of neuronal McSA1-IR within this region was considerably lower than that observed in the MTL. Interestingly, we noted that this unique case corresponded to one of the oldest subjects. The age- and region-dependent increase in iAβ appears to parallel some of the defining features of the AD continuum: regions most susceptible to the early disease process, such as the MTL, exhibit higher levels of iAβ, while those regions that are least-affected, such as the cerebellum, are burdened with considerably less iAβ material. Progressive iAβ accumulation may contribute to early synaptic dysfunction in brain regions implicated in the earliest stages of the AD pathology, such as the EC and hippocampus. While early iAβ buildup is sufficient to produce behavioral deficits in transgenic animal models, subtle cognitive impairment associated with progressive iAβ accumulation in humans may be masked by mechanisms that allow for cognitive reserve, such as neural compensation and neural reserve [67].

Oligomeric Aβ, which is thought to be the most potent, disease-relevant amyloid species [9, 77], has been shown to induce tau pathology [16, 73, 83], stimulate oxidative stress [15] and promote synaptic loss [38, 63]. However, these effects have mainly been studied in vitro following exogenous application of oligomeric Aβ, or in transgenic animal models. The progressive neuronal accumulation of soluble Aβ oligomers within the human brain has significant implications regarding the potential toxic effects of oligomeric Aβ during early disease stages. Using a conformation-specific monoclonal antibody, NU1 [42], we found that Aβ oligomers do in fact accumulate within the intraneuronal space in the post-mortem brain of non-demented subjects, in contrast with excellent previous reports [59], which may have been limited by the suboptimal preservation of conventional brain-bank materials. Given that soluble Aβ oligomers are thought to be the most toxic amyloid species compared with Aβ monomers and plaques, it is likely that more overt differences in the accumulation of oligomeric iAβ would be observed in patients with MCI or AD, who already exhibit cognitive symptoms; however, at present, we do not have access to tissue with comparable preservation from such a patient cohort. Several factors may favor the accumulation of Aβ oligomers in the intraneuronal space. The age-dependent increase in levels of Aβ may promote its spontaneous aggregation within the intracellular space, producing soluble, low-molecular weight oligomers that persist within the cytoplasm unless fluxed or degraded. The brain's ability to buffer the intracellular pool of oligomeric Aβ may also be influenced by factors subject to inter-individual variability, such as ApoE status, comorbidities, lifestyle and education.

Our findings also strongly indicate that there exists some relationship between the neuronal accumulation of soluble Aβ and the subsequent deposition of insoluble plaques. While the occurrence of iAβ was similar across most subjects, one case with more advanced Aβ plaque pathology exhibited a unique pattern of plaque deposition bearing striking similarities with the anatomical distribution of Aβ-burdened neurons in subjects devoid of Aβ plaques. Although this pattern of advanced plaque deposition has been documented in great detail [72], the sequential progression of insoluble plaque pathology in relation to the neuronal accumulation of soluble Aβ has never been considered. Considering that iAβ becomes established within AD-vulnerable brain regions before the deposition of Aβ plaques, it is possible that the age-dependent increase in iAβ causes a corresponding increase in the flux of Aβ peptides into the extracellular space, where they are prone to spontaneous aggregation. As a result, Aβ plaques may simply be the byproduct of neuronal homeostatic mechanisms that buffer increasing intracellular amyloid burden, explaining why brain plaque load naturally increases with age in both cognitively unimpaired and AD individuals. A larger cohort of cases displaying the complete continuum of plaque pathology would be necessary to study the dynamics between the intra- and extracellular amyloid pools.

Investigations into the role of iAβ in disease development have been hampered by criticisms about the technical limitations of IHC and conventional microscopy, as well as the challenges inherent to using post-mortem human brain tissue [70]. Varied reports on the ability to detect iAβ have also been muddied by inconsistent fixation and treatment methods across studies. These confounding factors may explain contradictory reports on the occurrence of intracellular Aβ oligomers in human neurons and post-mortem brain tissue [23, 59, 68]. Applying optimal perfusion and fixation protocols with short post-mortem delays resulted in extremely high-quality human brain material, which, combined with well-controlled IHC protocols, allowed for the reliable detection of iAβ peptides and oligomers. Given the unique perfusion and fixation method implemented in this study, procurement of more post-mortem samples with similar preservation would be necessary to replicate present findings, as well as investigate the occurrence and progression of iAβ pathology across the full spectrum of AD neuropathology, both in non-demented subjects and individuals diagnosed with AD. We also demonstrate that the intracellular Aβ-IR pool detected using the Aβ-specific monoclonal

antibody, McSA1, is spatially distinct from that associated with the APP/CTF-specific polyclonal antibody, pab27576. Using super resolution SIM to more accurately resolve the intracellular distribution of Aβ and APP/CTF, we demonstrate that only about 6% of McSA1-IR sites overlap with that of pab27576, and vice versa. McSA1-IR puncta were evenly distributed throughout the cell soma and dendrites, while pab27576-IR structures were much larger and more evenly distributed throughout all neuronal structures. Such striking differences in the distribution of both antibodies suggest that they do in fact target distinct peptides occurring in discrete cellular compartments. The lack of significant colocalization between the two antibodies confirms that the intracellular McSA1-IR pool is associated with neither APP nor CTF.

It has become widely acknowledged that neurons retain a soluble pool of Aβ peptides; however, information on the effects of progressive iAβ buildup within the human brain are lacking, despite substantial evidence that iAβ likely contributes to early disease development and drives the neurodegenerative mechanisms that culminate in Alzheimer's dementia. Our study reveals the presence of a neuronal pool of soluble Aβ that becomes established in AD-vulnerable brain regions before Aβ plaque deposition or tau hyperphosphorylation. The fact that iAβ is consistently detected within the non-demented human brain indicates that iAβ can be tolerated to some extent without producing cognitive symptoms. These results suggest that iAβ accumulation and oligomerization may in fact represent the earliest stage of the amyloid pathology, unleashing downstream mechanisms implicated in AD development, including oxidative stress, inflammation, tau hyperphosphorylation and synaptic dysfunction. Consequently, understanding the homeostatic threshold for iAβ and the mechanisms by which excessive iAβ accumulation elicits the AD pathological cascade may reveal more precise molecular targets amenable to early pharmacological intervention.

In sum, our study underscores the possibility that abnormal iAβ accumulation within the entorhinal cortex represents a primary pathogenic component of the amyloid cascade, triggering subsequent tau hyperphosphorylation and progressive tau pathology.

Acknowledgements This research is supported by the CIHR Project Grant PJT-364544 to A. Claudio Cuello, and 2017-1.2.1-NKP-2017-00002 to the Human Brain Research lab. LAW is the recipient of a Doctoral Training Fellowship from the Fonds de recherche du Québec-Santé. SDC is the holder of the Charles E. Frosst/Merck Research Associate position. ACC is the holder of the McGill University Charles E. Frosst/Merck Chair in Pharmacology and is a member of the Canadian Consortium on Neurodegeneration in Aging. We would like to thank Dr. William Klein (Northwestern University) as well as Dr. Gerhard Multhaup (McGill University) for generously providing the NU1 and pab27576 antibodies, respectively. We thank Dr. Alfredo Ribeiro-da-Silva for allowing us to use the Axio Imager M2 widefield microscope and for his guidance and assistance in acquiring the images presented above. We would also like to acknowledge Dr. Elke Küster-Schöck and the McGill University Cell Imaging and Analysis Network for their help with super resolution microscopy. The Cuello laboratory is grateful for the unrestricted support received from Dr. Alan Frosst, the Frosst family, and Merck Canada.

Compliance with ethical standards

Conflict of interest The authors declare that they have no conflict of interest.

References

1. Arriagada PV, Growdon JH, Hedley-Whyte ET, Hyman BT (1992) Neurofibrillary tangles but not senile plaques parallel duration and severity of Alzheimer's disease. Neurology 42:631–639
2. Bao F, Wicklund L, Lacor PN, Klein WL, Nordberg A, Marutle A (2012) Different beta-amyloid oligomer assemblies in Alzheimer brains correlate with age of disease onset and impaired cholinergic activity. Neurobiol Aging 33(825):e821
3. Billings LM, Oddo S, Green KN, McGaugh JL, LaFerla FM (2005) Intraneuronal Abeta causes the onset of early Alzheimer's disease-related cognitive deficits in transgenic mice. Neuron 45:675–688
4. Braak H, Alafuzoff I, Arzberger T, Kretzschmar H, Del Tredici K (2006) Staging of Alzheimer disease-associated neurofibrillary pathology using paraffin sections and immunocytochemistry. Acta Neuropathol 112:389–404
5. Braak H, Thal DR, Ghebremedhin E, Del Tredici K (2011) Stages of the pathologic process in Alzheimer disease: age categories from 1 to 100 years. J Neuropathol Exp Neurol 70:960–969
6. Busciglio J, Pelsman A, Wong C, Pigino G, Yuan M, Mori H, Yankner BA (2002) Altered metabolism of the amyloid beta precursor protein is associated with mitochondrial dysfunction in Down's syndrome. Neuron 33:677–688
7. Capetillo-Zarate E, Gracia L, Yu F, Banfelder JR, Lin MT, Tampellini D, Gouras GK (2011) High-resolution 3D reconstruction reveals intra-synaptic amyloid fibrils. Am J Pathol 179:2551–2558
8. Chui DH, Tanahashi H, Ozawa K, Ikeda S, Checler F, Ueda O, Suzuki H, Araki W, Inoue H, Shirotani K et al (1999) Transgenic mice with Alzheimer presenilin 1 mutations show accelerated neurodegeneration without amyloid plaque formation. Nat Med 5:560–564
9. Cline EN, Bicca MA, Viola KL, Klein WL (2018) The amyloid-beta oligomer hypothesis: beginning of the third decade. J Alzheimers Dis 18:1–43
10. Cohen RM, Rezai-Zadeh K, Weitz TM, Rentsendorj A, Gate D, Spivak I, Bholat Y, Vasilevko V, Glabe CG, Breunig JJ et al (2013) A transgenic Alzheimer rat with plaques, tau pathology, behavioral impairment, oligomeric abeta, and frank neuronal loss. J Neurosci 33:6245–6256
11. Cuello AC, Allard S, Ferretti MT (2012) Evidence for the accumulation of Abeta immunoreactive material in the human brain and in transgenic animal models. Life Sci 91:1141–1147
12. D'Andrea MR, Nagele RG, Gumula NA, Reiser PA, Polkovitch DA, Hertzog BM, Andrade-Gordon P (2002) Lipofuscin and Abeta42 exhibit distinct distribution patterns in normal and Alzheimer's disease brains. Neurosci Lett 323:45–49
13. D'Andrea MR, Nagele RG, Wang HY, Lee DH (2002) Consistent immunohistochemical detection of intracellular beta-amyloid42

in pyramidal neurons of Alzheimer's disease entorhinal cortex. Neurosci Lett 333:163–166
14. D'Andrea MR, Nagele RG, Wang HY, Peterson PA, Lee DH (2001) Evidence that neurones accumulating amyloid can undergo lysis to form amyloid plaques in Alzheimer's disease. Histopathology 38:120–134
15. De Felice FG, Velasco PT, Lambert MP, Viola K, Fernandez SJ, Ferreira ST, Klein WL (2007) Abeta oligomers induce neuronal oxidative stress through an *N*-methyl-D-aspartate receptor-dependent mechanism that is blocked by the Alzheimer drug memantine. J Biol Chem 282:11590–11601
16. De Felice FG, Wu D, Lambert MP, Fernandez SJ, Velasco PT, Lacor PN, Bigio EH, Jerecic J, Acton PJ, Shughrue PJ et al (2008) Alzheimer's disease-type neuronal tau hyperphosphorylation induced by A beta oligomers. Neurobiol Aging 29:1334–1347
17. DeKosky ST, Scheff SW (1990) Synapse loss in frontal cortex biopsies in Alzheimer's disease: correlation with cognitive severity. Ann Neurol 27:457–464
18. Do Carmo S, Crynen G, Paradis T, Reed J, Iulita MF, Ducatenzeiler A, Crawford F, Cuello AC (2018) Hippocampal proteomic analysis reveals distinct pathway deregulation profiles at early and late stages in a rat model of Alzheimer's-like amyloid pathology. Mol Neurobiol 55:3451–3476
19. Dodart JC, Bales KR, Gannon KS, Greene SJ, DeMattos RB, Mathis C, DeLong CA, Wu S, Wu X, Holtzman DM et al (2002) Immunization reverses memory deficits without reducing brain Abeta burden in Alzheimer's disease model. Nat Neurosci 5:452–457
20. Ferretti MT, Allard S, Partridge V, Ducatenzeiler A, Cuello AC (2012) Minocycline corrects early, pre-plaque neuroinflammation and inhibits BACE-1 in a transgenic model of Alzheimer's disease-like amyloid pathology. J Neuroinflammation 9:62
21. Ferretti MT, Partridge V, Leon WC, Canneva F, Allard S, Arvanitis DN, Vercauteren F, Houle D, Ducatenzeiler A, Klein WL et al (2011) Transgenic mice as a model of pre-clinical Alzheimer's disease. Curr Alzheimer Res 8:4–23
22. Fowler SW, Chiang AC, Savjani RR, Larson ME, Sherman MA, Schuler DR, Cirrito JR, Lesne SE, Jankowsky JL (2014) Genetic modulation of soluble Abeta rescues cognitive and synaptic impairment in a mouse model of Alzheimer's disease. J Neurosci 34:7871–7885
23. Goni F, Marta-Ariza M, Herline K, Peyser D, Boutajangout A, Mehta P, Drummond E, Prelli F, Wisniewski T (2018) Anti-beta-sheet conformation monoclonal antibody reduces tau and Abeta oligomer pathology in an Alzheimer's disease model. Alzheimers Res Ther 10:10
24. Gouras GK, Tampellini D, Takahashi RH, Capetillo-Zarate E (2010) Intraneuronal beta-amyloid accumulation and synapse pathology in Alzheimer's disease. Acta Neuropathol 119:523–541
25. Gouras GK, Tsai J, Naslund J, Vincent B, Edgar M, Checler F, Greenfield JP, Haroutunian V, Buxbaum JD, Xu H et al (2000) Intraneuronal Abeta42 accumulation in human brain. Am J Pathol 156:15–20
26. Gouras GK, Willen K, Tampellini D (2012) Critical role of intraneuronal Abeta in Alzheimer's disease: technical challenges in studying intracellular Abeta. Life Sci 91:1153–1158
27. Grant SM, Ducatenzeiler A, Szyf M, Cuello AC (2000) Abeta immunoreactive material is present in several intracellular compartments in transfected, neuronally differentiated, P19 cells expressing the human amyloid beta-protein precursor. J Alzheimers Dis 2:207–222
28. Gyure KA, Durham R, Stewart WF, Smialek JE, Troncoso JC (2001) Intraneuronal abeta-amyloid precedes development of amyloid plaques in Down syndrome. Arch Pathol Lab Med 125:489–492
29. Hanzel CE, Pichet-Binette A, Pimentel LS, Iulita MF, Allard S, Ducatenzeiler A, Do Carmo S, Cuello AC (2014) Neuronal driven pre-plaque inflammation in a transgenic rat model of Alzheimer's disease. Neurobiol Aging 35:2249–2262
30. Hardy J, Selkoe DJ (2002) The amyloid hypothesis of Alzheimer's disease: progress and problems on the road to therapeutics. Science 297:353–356
31. Iulita MF, Allard S, Richter L, Munter LM, Ducatenzeiler A, Weise C, Do Carmo S, Klein WL, Multhaup G, Cuello AC (2014) Intracellular Abeta pathology and early cognitive impairments in a transgenic rat overexpressing human amyloid precursor protein: a multidimensional study. Acta Neuropathol Commun 2:61
32. Jack CR Jr, Knopman DS, Jagust WJ, Petersen RC, Weiner MW, Aisen PS, Shaw LM, Vemuri P, Wiste HJ, Weigand SD et al (2013) Tracking pathophysiological processes in Alzheimer's disease: an updated hypothetical model of dynamic biomarkers. Lancet Neurol 12:207–216
33. Janelsins MC, Mastrangelo MA, Oddo S, LaFerla FM, Federoff HJ, Bowers WJ (2005) Early correlation of microglial activation with enhanced tumor necrosis factor-alpha and monocyte chemoattractant protein-1 expression specifically within the entorhinal cortex of triple transgenic Alzheimer's disease mice. J Neuroinflammation 2:23
34. Kaden D, Harmeier A, Weise C, Munter LM, Althoff V, Rost BR, Hildebrand PW, Schmitz D, Schaefer M, Lurz R et al (2012) Novel APP/Abeta mutation K16 N produces highly toxic heteromeric Abeta oligomers. EMBO Mol Med 4:647–659
35. Kalus P, Braak H, Braak E, Bohl J (1989) The presubicular region in Alzheimer's disease: topography of amyloid deposits and neurofibrillary changes. Brain Res 494:198–203
36. Kenigsberg RL, Cuello AC (1990) Production of a bi-specific monoclonal antibody recognizing mouse kappa light chains and horseradish peroxidase. Applications in immunoassays. Histochemistry 95:155–163
37. Koss DJ, Jones G, Cranston A, Gardner H, Kanaan NM, Platt B (2016) Soluble pre-fibrillar tau and beta-amyloid species emerge in early human Alzheimer's disease and track disease progression and cognitive decline. Acta Neuropathol 132:875–895
38. Lacor PN, Buniel MC, Furlow PW, Clemente AS, Velasco PT, Wood M, Viola KL, Klein WL (2007) Abeta oligomer-induced aberrations in synapse composition, shape, and density provide a molecular basis for loss of connectivity in Alzheimer's disease. J Neurosci 27:796–807
39. LaFerla FM, Green KN, Oddo S (2007) Intracellular amyloid-beta in Alzheimer's disease. Nat Rev Neurosci 8:499–509
40. LaFerla FM, Troncoso JC, Strickland DK, Kawas CH, Jay G (1997) Neuronal cell death in Alzheimer's disease correlates with apoE uptake and intracellular Abeta stabilization. J Clin Invest 100:310–320
41. Lambert MP, Barlow AK, Chromy BA, Edwards C, Freed R, Liosatos M, Morgan TE, Rozovsky I, Trommer B, Viola KL et al (1998) Diffusible, nonfibrillar ligands derived from Abeta1-42 are potent central nervous system neurotoxins. Proc Natl Acad Sci U S A 95:6448–6453
42. Lambert MP, Velasco PT, Chang L, Viola KL, Fernandez S, Lacor PN, Khuon D, Gong Y, Bigio EH, Shaw P et al (2007) Monoclonal antibodies that target pathological assemblies of Abeta. J Neurochem 100:23–35
43. Lemere CA, Blusztajn JK, Yamaguchi H, Wisniewski T, Saido TC, Selkoe DJ (1996) Sequence of deposition of heterogeneous amyloid beta-peptides and APO E in Down syndrome: implications for initial events in amyloid plaque formation. Neurobiol Dis 3:16–32
44. Leon WC, Canneva F, Partridge V, Allard S, Ferretti MT, DeWilde A, Vercauteren F, Atifeh R, Ducatenzeiler A, Klein W et al (2010) A novel transgenic rat model with a full Alzheimer's-like amyloid

pathology displays pre-plaque intracellular amyloid-beta-associated cognitive impairment. J Alzheimers Dis 20:113–126
45. Li QX, Maynard C, Cappai R, McLean CA, Cherny RA, Lynch T, Culvenor JG, Trevaskis J, Tanner JE, Bailey KA et al (1999) Intracellular accumulation of detergent-soluble amyloidogenic A beta fragment of Alzheimer's disease precursor protein in the hippocampus of aged transgenic mice. J Neurochem 72:2479–2487
46. Lue LF, Kuo YM, Roher AE, Brachova L, Shen Y, Sue L, Beach T, Kurth JH, Rydel RE, Rogers J (1999) Soluble amyloid beta peptide concentration as a predictor of synaptic change in Alzheimer's disease. Am J Pathol 155:853–862
47. Martino Adami PV, Quijano C, Magnani N, Galeano P, Evelson P, Cassina A, Do Carmo S, Leal MC, Castano EM, Cuello AC et al (2017) Synaptosomal bioenergetic defects are associated with cognitive impairment in a transgenic rat model of early Alzheimer's disease. J Cereb Blood Flow Metab 37:69–84
48. McLean CA, Cherny RA, Fraser FW, Fuller SJ, Smith MJ, Beyreuther K, Bush AI, Masters CL (1999) Soluble pool of Abeta amyloid as a determinant of severity of neurodegeneration in Alzheimer's disease. Ann Neurol 46:860–866
49. Mena R, Wischik CM, Novak M, Milstein C, Cuello AC (1991) A progressive deposition of paired helical filaments (PHF) in the brain characterizes the evolution of dementia in Alzheimer's disease. An immunocytochemical study with a monoclonal antibody against the PHF core. J Neuropathol Exp Neurol 50:474–490
50. Milstein C, Cuello AC (1983) Hybrid hybridomas and their use in immunohistochemistry. Nature 305:537–540
51. Mochizuki A, Tamaoka A, Shimohata A, Komatsuzaki Y, Shoji S (2000) Abeta42-positive non-pyramidal neurons around amyloid plaques in Alzheimer's disease. Lancet 355:42–43
52. Mori C, Spooner ET, Wisniewsk KE, Wisniewski TM, Yamaguch H, Saido TC, Tolan DR, Selkoe DJ, Lemere CA (2002) Intraneuronal Abeta42 accumulation in Down syndrome brain. Amyloid 9:88–102
53. Nguyen DH, Zhou T, Shu J, and Mao JH (2013). Quantifying chromogen intensity in immunohistochemistry via reciprocal intensity. Cancer InCytes 2(1):e. http://www.cancerincytes.org/currentissue/letterfromtheeditorinchief.html#!quantifying-chromogen-intensity-in-immunohistochemistry-/c1vds
54. Oddo S, Caccamo A, Shepherd JD, Murphy MP, Golde TE, Kayed R, Metherate R, Mattson MP, Akbari Y, LaFerla FM (2003) Triple-transgenic model of Alzheimer's disease with plaques and tangles: intracellular Abeta and synaptic dysfunction. Neuron 39:409–421
55. Prasher VP, Farrer MJ, Kessling AM, Fisher EM, West RJ, Barber PC, Butler AC (1998) Molecular mapping of Alzheimer-type dementia in Down's syndrome. Ann Neurol 43:380–383
56. Qi Y, Klyubin I, Harney SC, Hu N, Cullen WK, Grant MK, Steffen J, Wilson EN, Do Carmo S, Remy S et al (2014) Longitudinal testing of hippocampal plasticity reveals the onset and maintenance of endogenous human Ass-induced synaptic dysfunction in individual freely behaving pre-plaque transgenic rats: rapid reversal by anti-Ass agents. Acta Neuropathol Commun 2:175
57. Rumble B, Retallack R, Hilbich C, Simms G, Multhaup G, Martins R, Hockey A, Montgomery P, Beyreuther K, Masters CL (1989) Amyloid A4 protein and its precursor in Down's syndrome and Alzheimer's disease. N Engl J Med 320:1446–1452
58. Samuel W, Terry RD, DeTeresa R, Butters N, Masliah E (1994) Clinical correlates of cortical and nucleus basalis pathology in Alzheimer dementia. Arch Neurol 51:772–778
59. Savioz A, Giannakopoulos P, Herrmann FR, Klein WL, Kovari E, Bouras C, Giacobini E (2016) A study of abeta oligomers in the temporal cortex and cerebellum of patients with neuropathologically confirmed Alzheimer's disease compared to aged controls. Neurodegener Dis 16:398–406
60. Schermelleh L, Heintzmann R, Leonhardt H (2010) A guide to super-resolution fluorescence microscopy. J Cell Biol 190:165–175
61. Selkoe DJ, Hardy J (2016) The amyloid hypothesis of Alzheimer's disease at 25 years. EMBO Mol Med 8:595–608
62. Semenenko FM, Bramwell S, Sidebottom E, Cuello AC (1985) Development of a mouse antiperoxidase secreting hybridoma for use in the production of a mouse PAP complex for immunocytochemistry and as a parent cell line in the development of hybrid hybridomas. Histochemistry 83:405–408
63. Shankar GM, Bloodgood BL, Townsend M, Walsh DM, Selkoe DJ, Sabatini BL (2007) Natural oligomers of the Alzheimer amyloid-beta protein induce reversible synapse loss by modulating an NMDA-type glutamate receptor-dependent signaling pathway. J Neurosci 27:2866–2875
64. Shankar GM, Li S, Mehta TH, Garcia-Munoz A, Shepardson NE, Smith I, Brett FM, Farrell MA, Rowan MJ, Lemere CA et al (2008) Amyloid-beta protein dimers isolated directly from Alzheimer's brains impair synaptic plasticity and memory. Nat Med 14:837–842
65. Skovronsky DM, Doms RW, Lee VM (1998) Detection of a novel intraneuronal pool of insoluble amyloid beta protein that accumulates with time in culture. J Cell Biol 141:1031–1039
66. Spires-Jones TL, Mielke ML, Rozkalne A, Meyer-Luehmann M, de Calignon A, Bacskai BJ, Schenk D, Hyman BT (2009) Passive immunotherapy rapidly increases structural plasticity in a mouse model of Alzheimer disease. Neurobiol Dis 33:213–220
67. Stern Y, Habeck C, Moeller J, Scarmeas N, Anderson KE, Hilton HJ, Flynn J, Sackeim H, van Heertum R (2005) Brain networks associated with cognitive reserve in healthy young and old adults. Cereb Cortex 15:394–402
68. Takahashi RH, Almeida CG, Kearney PF, Yu F, Lin MT, Milner TA, Gouras GK (2004) Oligomerization of Alzheimer's beta-amyloid within processes and synapses of cultured neurons and brain. J Neurosci 24:3592–3599
69. Takahashi RH, Milner TA, Li F, Nam EE, Edgar MA, Yamaguchi H, Beal MF, Xu H, Greengard P, Gouras GK (2002) Intraneuronal Alzheimer abeta42 accumulates in multivesicular bodies and is associated with synaptic pathology. Am J Pathol 161:1869–1879
70. Takahashi RH, Nagao T, Gouras GK (2017) Plaque formation and the intraneuronal accumulation of beta-amyloid in Alzheimer's disease. Pathol Int 67:185–193
71. Thal DR, Rub U, Orantes M, Braak H (2002) Phases of A beta-deposition in the human brain and its relevance for the development of AD. Neurology 58:1791–1800
72. Thal DR, Rub U, Schultz C, Sassin I, Ghebremedhin E, Del Tredici K, Braak E, Braak H (2000) Sequence of Abeta-protein deposition in the human medial temporal lobe. J Neuropathol Exp Neurol 59:733–748
73. Tomiyama T, Matsuyama S, Iso H, Umeda T, Takuma H, Ohnishi K, Ishibashi K, Teraoka R, Sakama N, Yamashita T et al (2010) A mouse model of amyloid beta oligomers: their contribution to synaptic alteration, abnormal tau phosphorylation, glial activation, and neuronal loss in vivo. J Neurosci 30:4845–4856
74. Toth K, Eross L, Vajda J, Halasz P, Freund TF, Magloczky Z (2010) Loss and reorganization of calretinin-containing interneurons in the epileptic human hippocampus. Brain 133:2763–2777
75. Townsend M, Shankar GM, Mehta T, Walsh DM, Selkoe DJ (2006) Effects of secreted oligomers of amyloid beta-protein on hippocampal synaptic plasticity: a potent role for trimers. J Physiol 572:477–492
76. Turner RS, Suzuki N, Chyung AS, Younkin SG, Lee VM (1996) Amyloids beta40 and beta42 are generated intracellularly in cultured human neurons and their secretion increases with maturation. J Biol Chem 271:8966–8970

77. Walsh DM, Selkoe DJ (2004) Oligomers on the brain: the emerging role of soluble protein aggregates in neurodegeneration. Protein Pept Lett 11:213–228
78. Wegiel J, Wisniewski HM, Dziewiatkowski J, Badmajew E, Tarnawski M, Reisberg B, Mlodzik B, De Leon MJ, Miller DC (1999) Cerebellar atrophy in Alzheimer's disease-clinicopathological correlations. Brain Res 818:41–50
79. Wertkin AM, Turner RS, Pleasure SJ, Golde TE, Younkin SG, Trojanowski JQ, Lee VM (1993) Human neurons derived from a teratocarcinoma cell line express solely the 695-amino acid amyloid precursor protein and produce intracellular beta-amyloid or A4 peptides. Proc Natl Acad Sci USA 90:9513–9517
80. Wirths O, Multhaup G, Czech C, Blanchard V, Moussaoui S, Tremp G, Pradier L, Beyreuther K, Bayer TA (2001) Intraneuronal Abeta accumulation precedes plaque formation in beta-amyloid precursor protein and presenilin-1 double-transgenic mice. Neurosci Lett 306:116–120
81. Wischik CM, Novak M, Thogersen HC, Edwards PC, Runswick MJ, Jakes R, Walker JE, Milstein C, Roth M, Klug A (1988) Isolation of a fragment of tau derived from the core of the paired helical filament of Alzheimer disease. Proc Natl Acad Sci USA 85:4506–4510
82. Wisniewski HM, Sadowski M, Jakubowska-Sadowska K, Tarnawski M, Wegiel J (1998) Diffuse, lake-like amyloid-beta deposits in the parvopyramidal layer of the presubiculum in Alzheimer disease. J Neuropathol Exp Neurol 57:674–683
83. Zempel H, Thies E, Mandelkow E, Mandelkow EM (2010) Abeta oligomers cause localized Ca(2+) elevation, missorting of endogenous Tau into dendrites, Tau phosphorylation, and destruction of microtubules and spines. J Neurosci 30:11938–11950